

$wR = 0.051$, 1534 measured reflections, 946 observed reflections ($I > 3.0\sigma(I)$), 83 refined parameters. Crystallographic data (excluding structure factors) for the structure reported in this paper have been deposited with the Cambridge Crystallographic Data Centre as supplementary publication no. CCDC-146823. Copies of the data can be obtained free of charge on application to CCDC, 12 Union Road, Cambridge CB2 1EZ, UK (fax: (+44) 1223-336-033; e-mail: deposit@ccdc.cam.ac.uk).

- [14] Elemental analysis of $\text{I}_2 \cdot \text{AuI}_2$ [%]: calcd for $\text{C}_{14}\text{H}_8\text{S}_4\text{Se}_8\text{AuI}_2$: C 12.12, H 0.58; found: C 12.63, H 0.84.
- [15] T. Mori, A. Kobayashi, Y. Sasaki, H. Kobayashi, G. Saito, H. Inokuchi, *Bull. Chem. Soc. Jpn.* **1984**, 57, 627–633. In the calculation of overlap integrals, the parameters for chalcogen atoms reported in reference [7c] were used.

Synthesis of $[(\text{Cp}^*\text{Re})_2\text{B}_n\text{H}_n]$ $n = 8-10$: Metal Boride Particles That Stretch the Cluster Structure Paradigms**

Sundargopal Ghosh, Maoyu Shang, Yaping Li, and Thomas P. Fehlner*

Metal borides are substances of considerable interest because of their physical, chemical, and electrical properties.^[1–4] Their simple stoichiometries belie complex extended structures and consequently, metal borides are rarely treated in basic inorganic texts. Yet, it was from metal borides that a solution to the molecular borane cluster structure problem arose, for example, CaB_6 formulated as a Zintl phase $[\text{Ca}^{2+}][\text{B}_6^{2-}]$ with a three-dimensional network of octahedral B_6 cages^[5] comparable with discrete $[\text{B}_6\text{H}_6^{2-}]$ ions.^[6] At the other end of the compositional scale, metal clusters with interstitial boron atoms have been identified which have the local bonding environment of boron in metal-rich borides.^[7] However, the borides of intermediate compositions, for example, CrB_4 ^[8], find no models in the molecular world. To date there has been no need to invoke a comparison as nearly all known metallaboranes contain late transition metal fragments and follow the same structural paradigm as the boranes.^[9, 10] Indeed it is a measure of the success of the cluster-electron counting rules and the isolobal analogy that boranes, metallaboranes, and metal clusters are linked in such a simple, conceptually pleasing, fashion.^[11–14]

Recently we discovered a few unusual compounds that do not fit the mold of the borane paradigm.^[15] Compared with

compounds containing later transition metal fragments, these compounds exhibit structures characterized by high metal-coordination number, cross-cluster bonds, and unexpected stability for low valent Group 6 and 7 metal compounds. In trying to understand the cause of this behavior we adopted an approach which has been usefully applied to borides of intermediate stoichiometries.^[16] Burdett and co-workers have pointed out that information on electronic structure is revealed by the change in structure with metal type at constant stoichiometry.^[17, 18] Specifically, for MB_2 and MB_4 borides (where M = metal) they demonstrated a correlation between the occupation of orbitals of MM and MB antibonding character and observed structure variation. In going from late to early transition metals, the metal-atom coordination number increases and the extent of MM and MB bonding increases. For $[(\text{Cp}^*\text{WH})_2\text{B}_7\text{H}_7]$, $[(\text{Cp}^*\text{Re})_2\text{B}_7\text{H}_7]$, and $[(\text{Cp}^*\text{W})_3\text{HB}_8\text{H}_8]$, we argued that in moving from late to earlier transition metals the geometric deviations from the cluster shapes of borane chemistry reflect a similar transition from electronic structures characteristic of boranes to those characteristic of borides.

An unconventional view based on three compounds constitutes an interesting curiosity rather than a useful idea. In further support we can now offer the characterization of a homologous series of metallaboranes that begins with $[(\text{Cp}^*\text{Re})_2\text{B}_7\text{H}_7]$. These compounds establish a new set of cluster geometries remarkably different from the canonical deltahedra of the $[\text{B}_n\text{H}_n]^{2-}$ boranes that underpin the cluster-electron counting rules.^[19, 20] The oblate cluster shapes, high metal-coordination numbers, and cross-cluster bonds featured support the idea that variation in the transition metal can drive a change from borane- to boride-like bonding.

Subsequent to the isolation of $[(\text{Cp}^*\text{Re})_2\text{B}_7\text{H}_7]$ from the reaction of $[\text{Cp}^*\text{ReCl}_4]$ and monoboranes,^[15] we found that it is formed in a more straightforward manner from the reaction of $[(\text{Cp}^*\text{ReH}_2)_2\text{B}_4\text{H}_4]$ with BH_3THF .^[21] Further development of this reaction permits the compounds $[(\text{Cp}^*\text{Re})_2\text{B}_n\text{H}_n]$, $n = 8-10$, to be isolated and characterized. Although produced in a mixture, they are insensitive to air and moisture and can be separated by thin layer chromatography (TLC) on the laboratory bench. Reactions of pure $[(\text{Cp}^*\text{Re})_2\text{B}_n\text{H}_n]$, $n = 7-10$, with BH_3THF demonstrate sequential cluster build up. So far all efforts to produce a compound with $n > 10$ have failed.

The molecular structures of the new compounds in the solid state,^[22] are shown in Figures 1–3. $[(\text{Cp}^*\text{Re})_2\text{B}_8\text{H}_8]$ possesses a C_2 axis bisecting the B1-B2 and B5-B6 edges (See also Figure 4). Three ^{11}B resonances in the intensity ratio 2:4:2 are observed by solution NMR spectroscopy in the temperature range -90 to 22°C suggesting accidental overlap of two signals or a low-barrier fluxional process in solution. The complex $[(\text{Cp}^*\text{Re})_2\text{B}_9\text{H}_9]$ possesses a plane of symmetry passing through the Re atoms and B5 consistent with the ^{11}B resonances (2:2:2:1) in solution NMR spectroscopy. The complex $[(\text{Cp}^*\text{Re})_2\text{B}_{10}\text{H}_{10}]$ possesses a C_2 axis bisecting the B2-B3 and B7-B8 edges consistent with the observed ^{11}B resonances (2:2:2:2). The wide range of boron chemical shifts and some uncharacteristically upfield terminal BH resonance signals constitutes the NMR signature of this

[*] Prof. T. P. Fehlner, Dr. S. Ghosh, Dr. M. Shang
Department of Chemistry and Biochemistry
University of Notre Dame
Notre Dame, IN 46556 (USA)
Fax: (+1) 219-631-6652
E-mail: fehlner.1@nd.edu

Dr. Y. Li
Department of Civil Engineering and Geological Sciences
University of Notre Dame
Notre Dame, IN 46556 (USA)

[**] This work was supported by the National Science Foundation. Cp = $\eta^5\text{-C}_5\text{Me}_5$.

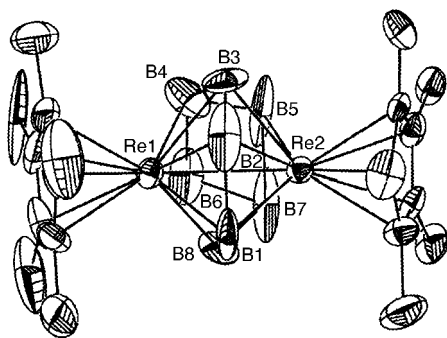


Figure 1. Molecular structure of $[(\text{Cp}^*\text{Re})_2\text{B}_8\text{H}_8]$. Selected distances [\AA]: Re1-B2 2.04(3), Re1-B1 2.09(3), Re1-B8 2.16(2), Re1-B4 2.211(19), Re1-B3 2.27(3), Re1-B6 2.33(3), Re1-Re2 2.8345(8), Re2-B2 2.05(2), Re2-B1 2.076(18), Re2-B7 2.19(2), Re2-B3 2.21(2), Re2-B5 2.31(2), Re2-B8 2.35(3), B1-B2 1.82(5), B1-B8 1.94(5), B2-B3 1.65(4), B3-B4 1.76(5), B3...B5 2.18(5), B4-B5 1.55(3), B4-B6 1.74(4), B5-B7 1.89(5), B5-B6 2.03(5), B6-B7 1.73(4), B6...B8 2.02(5), B7-B8 1.66(5).

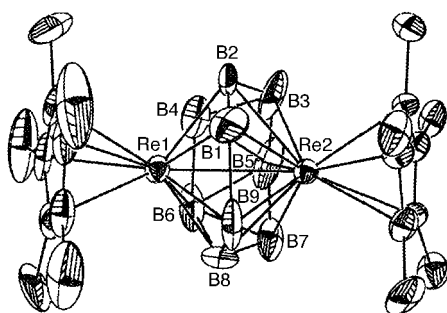


Figure 2. Molecular structure of $[(\text{Cp}^*\text{Re})_2\text{B}_9\text{H}_9]$. Selected distances [\AA]: Re1-B1 1.982(14), Re1-B9 2.075(12), Re1-B8 2.187(14), Re1-B6 2.209(12), Re1-B4 2.212(14), Re1-B2 2.216(15), Re1-Re2 2.8604(5), Re2-B9 2.165(11), Re2-B1 2.198(11), Re2-B3 2.215(13), Re2-B7 2.217(14), Re2-B5 2.299(16), Re2-B2 2.336(11), Re2-B8 2.402(13), B1-B2 1.70(2), B1-B9 1.869(18), B2-B3 1.70(2), B2-B4 1.83(3), B3-B5 1.55(2), B3-B4 1.63(2), B4-B6 1.86(2), B4-B5 1.858(18), B5-B7 1.67(2), B5-B6 1.86(2), B6-B7 1.736(19), B6-B8 1.82(2), B7-B8 1.646(19), B8-B9 1.794(17).

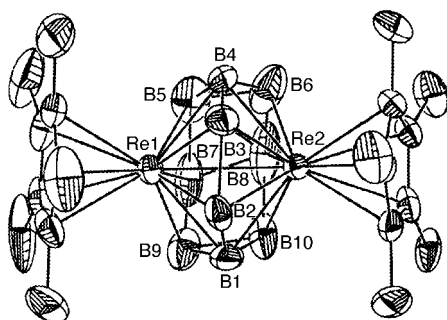


Figure 3. Molecular structure of $[(\text{Cp}^*\text{Re})_2\text{B}_{10}\text{H}_{10}]$. Selected distances [\AA]: Re1-B2 2.120(14), Re1-B3 2.185(15), Re1-B4 2.248(14), Re1-B9 2.268(17), Re1-B1 2.271(18), Re1-B5 2.272(17), Re1-B7 2.408(18), Re2-B3 2.131(13), Re2-B6 2.18(2), Re2-B2 2.190(13), Re2-B4 2.226(15), Re2-B1 2.226(14), Re2-B8 2.31(2), B1-B2 1.67(2), B1-B9 1.72(3), B1-B10 1.83(3), B2-B3 1.747(19), B3-B4 1.67(3), B4-B6 1.58(3), B4-B5 1.74(3), B5-B6 1.59(3), B5-B7 1.78(3), B5-B8 1.93(3), B6-B8 1.52(4), B7-B9 1.65(3), B7-B8 1.67(3), B7...B10 2.02(3), B8-B10 1.79(4), B9-B10 1.62(2).

structure type. The Re atoms occupy two vertices of connectivity 6 in $[(\text{Cp}^*\text{Re})_2\text{B}_8\text{H}_8]$, one vertex of connectivity 6 and one of connectivity 7 in $[(\text{Cp}^*\text{Re})_2\text{B}_9\text{H}_9]$, and two of connectivity 7 in $[(\text{Cp}^*\text{Re})_2\text{B}_{10}\text{H}_{10}]$. Each compound also

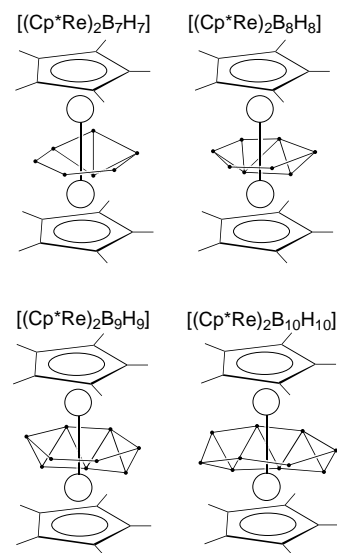


Figure 4. Structural representation of $[(\text{Cp}^*\text{Re})_2\text{B}_n\text{H}_n]$, $n = 7-10$, with heteronuclear bonding deleted. Open circles = Re, closed circles = BH.

contains a cross-cluster Re–Re bond ($d_{\text{Re-Re}}$ lies between 2.82 and 2.86 \AA).

As the Cp^*Re fragment is formally a 0-electron contributor to cluster bonding each of these clusters has $p-2$ sep (skeletal electron pairs) rather than the $p+1$ sep required for a normal deltahedral *closo* borane with p vertices, for example $[(\text{CpNi})_2\text{B}_n\text{H}_n]$, $n = 8, 10$ ($\text{Cp} = \text{C}_5\text{H}_5$).^[23, 24] Neither the capping nor cluster-fusion principles account for the structures of these hypoelectronic metallaboranes.^[14] Diamond–square–diamond (dsd) rearrangements (illustrated for $[(\text{Cp}^*\text{Re})_2\text{B}_8\text{H}_8]$, in Figure 5) convert the canonical geometries into those observed for $[(\text{Cp}^*\text{Re})_2\text{B}_n\text{H}_n]$, $n = 7-10$. In such a rearrangement the number of bonded edges remains constant but vertices of higher connectivity are generated, for example, for $n = 8$ (bicapped square antiprism) four vertices of connectivity 5 are converted into two vertices of connectivity 6 and two of connectivity 4 in the observed structure.

As a necessary consequence, the spherical canonical cluster becomes oblate with a relatively short cross-cluster distance between the high-coordinate vertices. The metal atoms occupy these vertices and the short cross-cluster distance permits the formation of an Re–Re bond. In going from the canonical structure to the observed structure B–B bonding is lost and replaced with M–B and M–M bonding,

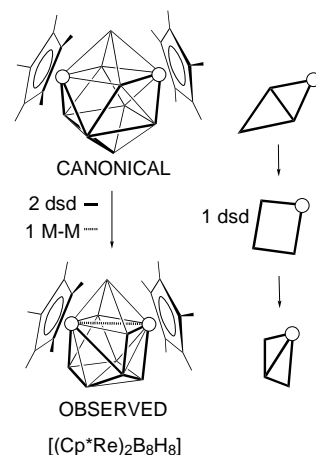


Figure 5. Generation of the observed structure of $[(\text{Cp}^*\text{Re})_2\text{B}_8\text{H}_8]$ from a bicapped square-antiprismatic cluster by two diamond–square–diamond (dsd) rearrangements (bold lines). The Re–Re bond is indicated by the dashed line and one dsd rearrangement is shown on the right.

for example, the pentagonal antiprism of the borane fragment of $[(\text{Cp}^*\text{Re})_2\text{B}_{10}\text{H}_{10}]$ in the canonical icosahedral form has become partially unraveled in the observed structure (Figure 6). Considering the robust nature of icosahedral boranes and carboranes, the dominance of transition metal bonding over main group bonding in these boron-rich compounds is surprising.

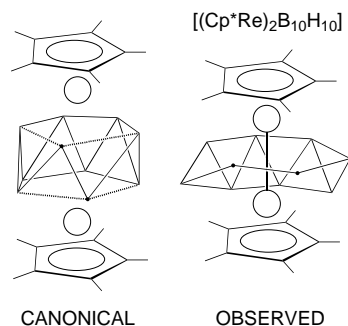


Figure 6. Loss of B–B bonding in the conversion of an icosahedral cluster shape into that observed for $[(\text{Cp}^*\text{Re})_2\text{B}_{10}\text{H}_{10}]$; lost bonds are shown by the dashed lines.

The compound $[(\text{Cp}^*\text{Re})_2\text{B}_6\text{H}_6]$ can be considered the parent member of the $[(\text{Cp}^*\text{Re})_2\text{B}_n\text{H}_n]$ series. Although this compound is unknown, the isolobal compounds $[(\text{Cp}^*\text{Re})_2\{\mu\text{-}\eta^6\text{-}\eta^6\text{-B}_4\text{H}_4\text{Co}_2(\text{CO})_5\}]^{[25]}$ and $[(\text{Cp}^*\text{Cr})_2\{\mu\text{-}\eta^6\text{-}\eta^6\text{-C}_3\text{H}_6\text{C}_2\text{B}_4\text{H}_4\}]^{[26]}$ with cross-cluster M–M bonds have been characterized. These compounds are triple-decker complexes^[27] and they provide insight on the electronic origin of the shapes observed. Comparing 9 sep $[(\text{Cp}^*\text{Rh})_2\{\mu\text{-}\eta^6\text{-}\eta^6\text{-C}_4\text{H}_4\text{B}_2\text{Me}_2\}]^{[2+][28]}$ with 6 sep $[(\text{Cp}^*\text{Re})_2\{\mu\text{-}\eta^6\text{-}\eta^6\text{-B}_6\text{H}_6\}]$ shows that as the Cp^*M fragments are moved within bonding distance three orbitals, which are filled in the 9 sep compound, are emptied and a substantial HOMO–LUMO gap is produced for 6 sep.^[29] Likewise, the generation of the observed structure of $[(\text{Cp}^*\text{Re})_2\text{B}_7\text{H}_7]$ from the canonical tricapped trigonal prismatic geometry causes three orbitals to rise sufficiently high in energy to become unoccupied.^[15, 30] As with the triple-decker complexes, these molecular orbitals consist of an ReRe antibonding orbital and two ReB orbitals that are boron-ring–metal δ antibonding. The ring orbitals emptied are also BB bonding which is consistent with decreased B–B bonding. In essence, the low electron count of the metal center demands additional bonding which is satisfied by a nonspherical shape at the expense of some B–B bonding. Like the metal borides of intermediate composition, an earlier transition metal fragment creates electronic requirements that are expressed in structural features not previously observed for boranes or metallaboranes containing later transition metal fragments.

Experimental Section

$[(\text{Cp}^*\text{Re})_2\text{B}_n\text{H}_n]$: $\text{BH}_3 \cdot \text{THF}$ (8-fold excess) was slowly added to a 100 mL Schlenk tube containing $[(\text{Cp}^*\text{ReH}_2)_2\text{B}_4\text{H}_4]$ (0.15 g, 0.21 mmol) in toluene (15 mL). The mixture was heated for 26 h at 90 °C, volatiles were removed in vacuo, the residue extracted in hexane: CH_2Cl_2 (9:1 v/v), and filtered through Celite. After removal of solvent from the filtrate, the residue was subjected to chromatographic work-up using silica gel TLC plates. Elution

with hexane: CH_2Cl_2 (8:2 v/v) yielded four closely spaced bands: yellow, $R_f=0.23$, $[(\text{Cp}^*\text{Re})_2\text{B}_7\text{H}_7]$ (0.02 g, 17%); orange-red, $R_f=0.14$, $[(\text{Cp}^*\text{Re})_2\text{B}_8\text{H}_8]$ (0.05 g, 38%); red, $R_f=0.09$, $[(\text{Cp}^*\text{Re})_2\text{B}_9\text{H}_9]$ (0.01 g, 10%); yellow, $R_f=0.05$, $[(\text{Cp}^*\text{Re})_2\text{B}_{10}\text{H}_{10}]$ (0.01 g, 7%). X-ray quality crystals were grown by slow diffusion of a hexane: CH_2Cl_2 (9:1 v/v) solution of $[(\text{Cp}^*\text{Re})_2\text{B}_n\text{H}_n]$ ($n=8-10$) at 5 °C. Selected data for $[(\text{Cp}^*\text{Re})_2\text{B}_n\text{H}_n]$, $n=8$: MS (EI): $[M^+]$ (max) = 736 (isotopic pattern for 2 Re and 8 B atoms), $^{12}\text{C}_{20}\text{H}_{38}\text{B}_8\text{Re}_2$, calcd: 739.2755; found: 739.2722 (exact mass measurement on $[M^+ - 1]$); ^{11}B NMR (C_6D_6 , 22 °C, 96 MHz): $\delta=97.92$ (d, $^1J(\text{B,H})=163$ Hz, 2B), 65.76 (d, $^1J(\text{B,H})=136$ Hz, 4B), 21.92 (d, $^1J(\text{B,H})=141$ Hz, 2B); ^1H NMR (C_6D_6 , 22 °C, 300 MHz): $\delta=9.86$ (partially collapsed quartet (pcq), 2BHr (t = terminal)), 9.02 (pcq, 4BHr), 1.86 (s, 30H, 2Cp*), 0.32 (pcq, 2BHr); IR (CH_2Cl_2 , cm^{-1}): 2521 w, 2443 w (B–Hr). $n=9$: MS (EI): $[M^+]$ (max) = 748 (isotopic pattern for 2 Re and 9 B atoms) $^{12}\text{C}_{20}\text{H}_{39}\text{B}_9\text{Re}_2$, calcd: 51.2926; found: 751.2908 (exact mass measurement on $[M^+ - 1]$); ^{11}B NMR (C_6D_6 , 22 °C): $\delta=94.08$ (d, $^1J(\text{B,H})=168$ Hz, 2B), 76.19 (d, $^1J(\text{B,H})=153$ Hz, 2B), 35.49 (d, $^1J(\text{B,H})=129$ Hz, 2B), 1.09 (d, $^1J(\text{B,H})=130$ Hz, 2B), -28.73 (d, $^1J(\text{B,H})=130$ Hz, 1B); ^1H NMR (C_6D_6 , 22 °C): $\delta=11.21$ (pcq, 2BHr), 10.23 (pcq, 2BHr), 8.46 (pcq, 2BHr), 1.92 (s, 15H, 1Cp*), 1.51 (s, 15H, 1Cp*), -0.12 (pcq, 2BHr), -2.26 (pcq, 1BHr); IR (CH_2Cl_2 , cm^{-1}): $\tilde{\nu}=2532$ w, 2430 w (B–Hr). $n=10$: MS (EI): $[M^+]$ (max) = 760 (isotopic pattern for 2 Re and 10 B atoms) $^{12}\text{C}_{20}\text{H}_{40}\text{B}_{10}\text{Re}_2$, calcd: 763.3098; found: 763.3126 (exact mass measurement on $[M^+ - 1]$); ^{11}B NMR (C_6D_6 , 22 °C): $\delta=59.95$ (d, $^1J(\text{B,H})=175$ Hz, 2B), 50.39 (d, $^1J(\text{B,H})=158$ Hz, 2B), 16.14 (d, $^1J(\text{B,H})=135$ Hz, 2B), -10.77 (d, $^1J(\text{B,H})=144$ Hz, 2B), -22.91 (d, $^1J(\text{B,H})=132$ Hz, 1B); ^1H NMR (C_6D_6 , 22 °C): $\delta=8.56$ (pcq, 2BHr), 6.84 (pcq, 2BHr), 5.96 (pcq, 2BHr), 1.43 (s, 30H, 2Cp*), 0.28 (pcq, 2BHr), -1.75 (pcq, 2BHr); IR (CH_2Cl_2 , cm^{-1}): $\tilde{\nu}=2531$ w, 2451 w (B–H).

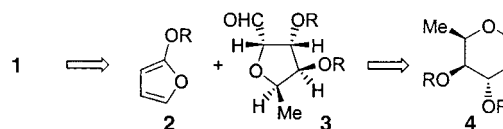
Received: November 8, 2000 [Z16056]

- [1] N. N. Greenwood, R. V. Parish, P. Thorton, *Q. Rev.* **1966**, *20*, 441.
- [2] R. Thompson in *Progress in Boron Chemistry*, Vol. 2 (Eds.: R. J. Brotherton, H. Steinberg) Pergamon, New York, **1970**.
- [3] V. I. Matkovich, *Pure Appl. Chem.* **1974**, *39*, 525.
- [4] T. Lundström in *Boron and Refractory Borides* (Ed.: V. I. Matkovich), Springer, Berlin, **1977**.
- [5] H. C. Longuet-Higgins, M. D. Roberts, *Proc. R. Soc. London A* **1955**, *230*, 110.
- [6] J. L. Boone, *J. Am. Chem. Soc.* **1964**, *86*, 5036.
- [7] C. E. Housecroft, *Adv. Organomet. Chem.* **1991**, *33*, 1.
- [8] S. Andersson, T. Lundström, *Acta Chem. Scand.* **1968**, *22*, 3103.
- [9] J. D. Kennedy, *Prog. Inorg. Chem.* **1984**, *32*, 519.
- [10] J. D. Kennedy, *Prog. Inorg. Chem.* **1986**, *34*, 211.
- [11] K. Wade, *Inorg. Nucl. Chem. Lett.* **1972**, *8*, 559.
- [12] K. Wade, *Adv. Inorg. Chem. Radiochem.* **1976**, *18*, 1.
- [13] D. M. P. Mingos, *Nature Phys. Sci.* **1972**, *236*, 99.
- [14] D. M. P. Mingos, D. J. Wales, *Introduction to Cluster Chemistry*, Prentice Hall, New York, **1990**.
- [15] A. S. Weller, M. Shang, T. P. Fehlner, *Organometallics* **1999**, *18*, 853.
- [16] T. P. Fehlner, *J. Solid State Chem.* **2000**, *154*, 110.
- [17] J. K. Burdett, E. Canadell, G. J. Miller, *J. Am. Chem. Soc.* **1986**, *108*, 6561.
- [18] J. K. Burdett, E. Canadell, *Inorg. Chem.* **1988**, *27*, 4437.
- [19] R. E. Williams, *Inorg. Chem.* **1971**, *10*, 210.
- [20] R. W. Rudolph, *Acc. Chem. Res.* **1976**, *9*, 446.
- [21] S. Ghosh, X. Lei, M. Shang, T. P. Fehlner, *Inorg. Chem.* **2000**, *39*, 5373.
- [22] Crystallographic data (excluding structure factors) for the structures reported in this paper have been deposited with the Cambridge Crystallographic Data Centre as supplementary publication no. CCDC-151686, CCDC-151687, and CCDC-151688. Copies of the data can be obtained free of charge on application to CCDC, 12 Union Road, Cambridge CB21EZ, UK (fax: (+44) 1223-336-033; e-mail: deposit@ccdc.cam.ac.uk).
- [23] J. R. Bowser, A. Bonny, J. R. Pipal, R. N. Grimes, *J. Am. Chem. Soc.* **1979**, *101*, 6229.
- [24] R. N. Leyden, B. P. Sullivan, R. T. Baker, M. F. Hawthorne, *J. Am. Chem. Soc.* **1978**, *100*, 3758.
- [25] S. Ghosh, M. Shang, T. P. Fehlner, *J. Am. Chem. Soc.* **1999**, *121*, 7451.

- [26] K. Kawamura, M. Shang, O. Wiest, T. P. Fehlner, *Inorg. Chem.* **1998**, 37, 608.
 [27] G. E. Herberich in *Comprehensive Organometallic Chemistry II, Vol. 1* (Eds.: E. Abel, F. G. A. Stone, G. Wilkinson), Pergamon, Oxford, **1995**, p. 197.
 [28] G. E. Herberich, B. Hessner, G. Huttner, L. Zsolnai, *Angew. Chem.* **1981**, 93, 471; *Angew. Chem. Int. Ed. Engl.* **1981**, 20, 472.
 [29] E. D. Jemmis, A. C. Reddy, *Organometallics* **1988**, 7, 1561.
 [30] A. S. Weller, M. Shang, T. P. Fehlner, *Chem. Commun.* **1998**, 1787.

struction of highly oxygenated tetrahydrofurans from glycal starting materials is reported.

Initial retrosynthetic disconnection of **1** (Scheme 1) leads back to a 2-alkoxyfuran **2** and the highly oxygenated tetrahydrofurfural derivative **3** as viable synthetic precursors.



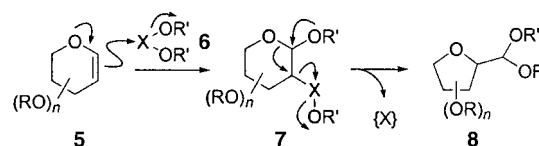
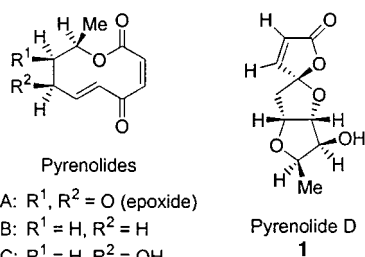
Scheme 1. Retrosynthetic analysis.

Total Synthesis of (+)-Pyrenolide D**

Kenneth M. Engstrom, Mario R. Mendoza, Mauricio Navarro-Villalobos, and David Y. Gin*

The phylogenetic fungus *Pyrenophora teres* has been a source of a number of fungal metabolites of interesting and varying biological activities. These metabolites include the pyrenolides A–C,^[1] simple macrocyclic lactones that exhibit potent

Although a number of synthetic strategies to prepare **3** can be envisioned through the synthesis and cyclization of acyclic polyol precursors, we reasoned that a more efficient approach might arise from a stereoselective oxidative ring contraction of a glycal substrate such as 6-deoxy-D-gulal (**4**), incorporating three of the four stereocenters within **3**. For such an oxidative ring contraction process to be feasible, an appropriate electrophilic oxidant **6** (Scheme 2) is required. Not only must



Scheme 2. Oxidative ring contraction of glycals.

growth-inhibitory and morphogenic activities toward fungi. A fourth metabolite, pyrenolide D (**1**),^[2] is structurally distinct from the other members of this family in that it incorporates a highly oxygenated tricyclic spiro- γ -lactone structure related to certain members of the cephalosporolide class of natural products.^[3] Moreover, pyrenolide D is further distinguished from the other pyrenolides in that it is not active toward fungi, but rather that it exhibits significant cytotoxic activity toward HL-60 cells. This biological profile, in combination with its densely functionalized polycyclic structure, spawned our efforts to develop a synthetic approach to **1** that would also establish the absolute configuration of the natural product. We report herein the first total synthesis of **1** by a very short sequence. In this context, a method for the efficient con-

this reagent efficiently perform an electrophilic activation of the glycal substrate (**5**→**7**), but it must also concomitantly install a potent leaving group at the C2 position of the activated pyranoside intermediate **7**. This would hopefully allow 1,2-migration of the endocyclic C–O bond in a displacement of the C2 leaving group, resulting in a net oxidative ring contraction of the glycal substrate to form the C-furanoside product **8**, an intermediate that directly maps onto the proposed synthetic intermediate **3** (Scheme 1). Given our interest in glycal activation processes,^[4] we sought to establish the means to effect the conversion of **5** into **8** as one of the key steps in the synthesis of **1**.

Based on this strategy, the initial synthetic target involved the preparation of 2,3-di-*O*-protected-6-deoxy-D-gulal (**4**) as the desired substrate for the formation of the C-furanoside **3**. The synthesis commenced (Scheme 3) with the preparation of the pseudoglycal **10** from commercially available tri-*O*-acetyl-D-galactal (**9**) through a three-step sequence that included: SnCl₄-catalyzed Ferrier-type glycosylation of thiophenol (84%), acetate hydrolysis and selective tosylation of the C6-hydroxy group (78%), and hydride displacement of the C6-sulfonate functionality (86%).^[5] Subsequent oxidation of the allylic sulfide in **10** with *m*-chloroperoxybenzoic acid led to the formation of the corresponding anomeric sulfoxide, which underwent an Evans–Mislow [2,3]-sigmatropic rearrangement. Subsequent aminolysis of the sulfenyl functionality installed the α -C3-OH group (89%).^[6] The resulting 6-deoxy-D-gulal diol **11** was protected as the bis(*tert*-butyldimethylsil-

[*] Prof. D. Y. Gin, K. M. Engstrom, M. R. Mendoza, Dr. M. Navarro-Villalobos
 Department of Chemistry, University of Illinois
 Urbana, IL 61801 (USA)
 Fax: (+1)217-244-8024
 E-mail: gin@scs.uiuc.edu

[**] This research was supported by the National Institutes of Health, Glaxo Wellcome Inc., the Alfred P. Sloan Foundation, and the Arnold and Mabel Beckman Foundation.

Supporting information for this article is available on the WWW under <http://www.angewandte.com> or from the author.